



Tau Isoform-Specific Modulation of Kinesin-Driven Microtubule Gliding Rates and Trajectories as Determined with Tau-Stabilized Microtubules

Austin Peck,^{1,2} M. Emre Sargin,³ Nichole E. LaPointe,^{1,2} Kenneth Rose,³ B. S. Manjunath,³ Stuart C. Feinstein,^{1,2} and Leslie Wilson^{1,2*}

¹Neuroscience Research Institute, University of California, Santa Barbara, California

²Department of Molecular, Cellular, and Developmental Biology, University of California, Santa Barbara, California

³Department of Electrical and Computer Engineering, University of California, Santa Barbara, California

Received 23 August 2010; Revised 1 October 2010; Accepted 1 October 2010
Monitoring Editor: George Bloom

We have utilized tau-assembled and tau-stabilized microtubules (MTs), in the absence of taxol, to investigate the effects of tau isoforms with three and four MT binding repeats upon kinesin-driven MT gliding. MTs were assembled in the presence of either 3-repeat tau (3R tau) or 4-repeat tau (4R tau) at tau:tubulin dimer molar ratios that approximate those found in neurons. MTs assembled with 3R tau glided at 31.1 $\mu\text{m}/\text{min}$ versus 25.8 $\mu\text{m}/\text{min}$ for 4R tau, a statistically significant 17% difference. Importantly, the gliding rates for either isoform did not change over a fourfold range of tau concentrations. Further, tau-assembled MTs underwent minimal dynamic instability behavior while gliding and moved with linear trajectories. In contrast, MTs assembled with taxol in the absence of tau displayed curved gliding trajectories. Interestingly, addition of 4R tau to taxol-stabilized MTs restored linear gliding, while addition of 3R tau did not. The data are consistent with the ideas that (i) 3R and 4R tau-assembled MTs possess at least some isoform-specific features that impact upon kinesin translocation, (ii) tau-assembled MTs possess different structural features than do taxol-assembled MTs, and (iii) some features of tau-assembled MTs can be masked by prior assembly by taxol. The differences in kinesin-driven gliding between 3R and 4R tau suggest important features of tau function related to the normal shift in tau isoform composition that occurs during neural development as well as in neurodegeneration caused by

altered expression ratios of otherwise normal tau isoforms. © 2010 Wiley-Liss, Inc.

Key Words: neurodegeneration, axonal transport, frontotemporal dementia, motor protein

Introduction

Tau is a neural microtubule (MT)-associated protein (MAP) that binds to MTs, promotes MT assembly, and regulates MT dynamics in the developing and adult nervous systems [Feinstein and Wilson, 2005]. Although there is only a single tau gene, alternative RNA splicing produces six tau isoforms, each possessing either three (3R tau) or four (4R tau) imperfect MT binding repeats located in the C-terminal half of the protein, and either zero, one, or two inserts located in the N-terminal portion of the protein (projection domain, Fig. 1), which is believed to extend outward from the MT surface [Hirokawa et al., 1988; Lee et al., 1988; Himmler et al., 1989; Himmler, 1989; Butner and Kirschner, 1991; Chen et al., 1992; Goode and Feinstein, 1994]. Whereas fetal brain expresses only the shortest 3R tau isoform, adult human brain expresses approximately equal amounts of the 3R tau and 4R tau isoforms [Kosik et al., 1989]. 4R tau generally exhibits higher levels of MT assembly promoting and dynamics regulatory activities than 3R tau [Goedert and Jakes, 1990; Trinczek et al., 1995; Goode et al., 2000; Panda et al., 2003; Bunker et al., 2004; Levy et al., 2005]. Qualitative mechanistic differences between 3R and 4R tau action have also been described [Levy et al., 2005]. The fact that 3R and 4R tau differentially regulate MT dynamics has given rise to a functional shift model in which 3R tau enables relatively dynamic MTs to exist during fetal axonal outgrowth, while 4R tau confers increased MT stability during adulthood after synaptic connections have been established [Kosik et al., 1989; Panda et al., 2003; Bunker et al., 2004; Feinstein and Wilson, 2005; Levy et al., 2005]. Elucidating the functional differences

Additional Supporting Information may be found in the online version of this article.

*Address correspondence to: Leslie Wilson, Department of Molecular, Cellular, and Developmental Biology, LSB 1119, University of California, Santa Barbara, CA 93106. E-mail: wilson@lifesci.ucsb.edu

Published online 10 November 2010 in Wiley Online Library (wileyonlinelibrary.com).

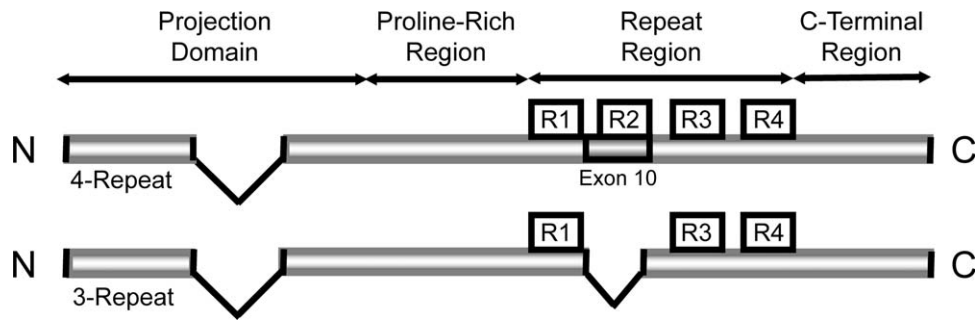


Fig. 1. Schematic of tau isoforms used in this work. These isoforms differ only by the presence (4R) or absence (3R) of the alternatively spliced exon 10, comprising repeat two (R2) and the inter-repeat between R1 and R2. Both isoforms lack the two alternatively spliced exons in the projection domain.

between 3R and 4R tau may also provide insight into how misregulation of the 3R to 4R tau expression ratio leads to neuronal cell death and dementia in a variety of tauopathies, including FTDP-17, PSP, and CBD, neurodegenerative diseases with many similarities to Alzheimer's disease [Lee et al., 2001; Stokin et al., 2005; Duncan and Goldstein, 2006; Ballatore et al., 2007].

Axonal transport is essential for the normal development and maintenance of the nervous system and aberrant axonal transport can cause neuronal cell death [Saxton et al., 1991; Ferreira et al., 1992; Hurd et al., 1996; Ebnet et al., 1998; Tanaka et al., 1998; Trinczek et al., 1999; LaMonte et al., 2002; Stamer et al., 2002; Mandelkowitz et al., 2003; Kieran et al., 2005; Stokin et al., 2005]. Because MTs serve as the tracks upon which axonal transport proceeds, and tau is a MT stabilizing MAP, the possible effects of tau upon axonal transport are important to understand. Several studies in neuronal cells support the notion that tau might regulate various aspects of kinesin activity. For example, overexpression of tau in cultured neuronal cells led to impaired axonal transport and organelle depletion in neuronal processes, enhanced oxidative stress in distal neuritic regions, and a net retrograde bias of dynein-associated cargo [Ebnet et al., 1998; Trinczek et al., 1999; Stamer et al., 2002; Mandelkowitz et al., 2003]. Also, overexpression of 4R tau in transgenic mice resulted in axonal degeneration and accumulation of mitochondria and vesicles in the cell soma [Spittaels et al., 1999]. In vitro, addition of tau to taxol-assembled MTs inhibited the docking of kinesin to the MTs [Seitz et al., 2002; Vershinin et al., 2007; Dixit et al., 2008] and decreased the kinesin run length [Vershinin et al., 2007; Dixit et al., 2008]. Interestingly, these effects of tau were not caused by the projection domain since the 3R tau isoform with the shortest projection domain (3R0N tau with no N-terminal exons) had more marked effects than 4R2N tau, which contains both N-terminal exons and has the longest projection domain [Vershinin et al., 2007; Dixit et al., 2008]. Especially relevant to the work reported here, addition of tau to taxol-stabilized MTs has been reported to have little effect on kinesin-translocation velocity [Trinc-

zek et al., 1999; Seitz et al., 2002; Morfini et al., 2007; Dixit et al., 2008].

In the foregoing studies, MTs were viewed as static, inert structures. However, MTs may not be simple passive substrates for MAPs and motors. For example, tau can alter the MT protofilament number [Choi et al., 2009]. Additionally, tau regulates MT dynamics at very low tau:tubulin molar ratios (as low as one tau molecule per several hundred tubulin dimers), despite the fact that tau is known to bind along the entire length of a MT. These observations are consistent with tau-induced allosteric effects upon MT structure [Panda et al., 1995]. Data also suggest that motors can affect MT structure. For example, cryo-electron microscopic analyses have revealed structural modifications in α -tubulin subunits in response to kinesin docking, leading to increased interdimer contact and increased axial stability along protofilaments [Krebs et al., 2004]. Further, kinesin binding to MTs appears to promote directionally biased, long-range cooperativity of subsequent motor binding, consistent with the notion that the MT may undergo conformational changes that facilitate transport [Muto et al., 2005]. MTs also change in response to taxol. Specifically, taxol alters MT diameter and protofilament number [Diaz et al., 1998], and taxol binding to MTs increases both longitudinal intradimer and lateral interdimer bond energies by imposing conformation restraints on both α - and β -tubulin subunits [Xiao et al., 2006]. Modeling based on the tubulin crystal structure predicts increased lateral contacts between adjacent protofilaments in response to the binding of docetaxel to MTs [Keskin et al., 2002]. Further, like tau, taxol suppresses MT dynamic instability at extremely low molar ratios of taxol:tubulin in MTs (as low as 1:1000), suggesting that small numbers of bound taxol molecules might stabilize MTs by inducing long range structural alterations in the lattice [Derry et al., 1995]. Thus, the use of taxol to stabilize MTs in in vitro assays could mask effects of tau and/or kinesin on MT surface topology that might be important in motor-driven motility.

Further complicating our understanding of how taxol might affect the ability of tau to regulate motor-based

transport is the fact that tau is able to bind to two distinct sites on MTs, one of which may overlap with the site for taxol. For many years, it has been widely held that tau binds to the acidic carboxyl termini of tubulin at the MT surface [Serrano et al., 1985; Melki et al., 1991; Redeker et al., 1992; Marya et al., 1994; Maccioni et al., 1995; Chau et al., 1998]. However, more recent work has indicated that there is a high affinity binding site for tau on the inner surface of the MT close to the taxol binding site [Nogales et al., 1995; Kar et al., 2003], and evidence suggests that tau and taxol may compete with one another for binding to MTs [Nogales et al., 1995; Al-Bassam et al., 2002; Kar et al., 2003; Samsonov et al., 2004; Park et al., 2008]. Indeed, tau and taxol exert similar effects upon MT dynamics [Derry et al., 1995; Panda et al., 1995; Bunker et al., 2004; Levy et al., 2005]. Thus, taxol might influence the binding of tau to MTs, which in turn could influence the effects of tau on motor-driven transport.

In this study, we used tau-stabilized MTs rather than taxol-stabilized MTs to ask whether 3R tau and 4R tau, which differentially stabilize MT dynamic instability, might also differentially modulate kinesin-driven gliding. We find that MTs assembled by 3R tau glide 17% faster than MTs assembled with 4R tau, a statistically significant difference. Importantly, this difference did not vary over a range of tau concentrations. Additionally using taxol-stabilized MTs, we also found that tau exerts isoform-specific effects on MT gliding trajectories. The differences in kinesin-driven motility with 3R and 4R tau may be important in neuronal development and maintenance and the onset and/or progression of neurodegenerative disease.

Materials and Methods

Tubulin Purification and Rhodamine Labeling

MAP-free tubulin dimers (>99% pure) were purified from bovine brain in the absence of any stabilizing agents as previously described [Miller and Wilson, 2010]. Rhodamine-labeled tubulin (0.7 mol rhodamine per mol tubulin) was prepared by carboxyrhodamine labeling (Molecular Probes) as described [Hyman et al., 1991].

Purification of Tau

Tau (>99% pure) was recombinantly produced using pRK expression vectors containing cDNA sequences encoding 3R0N or 4R0N tau (possessing either 3 or 4 MT binding repeats, and no N-terminal inserts) that were kind gifts from Drs. Kenneth Kosik (UC Santa Barbara) and Gloria Lee (Iowa State University). The constructs were expressed in BL21 (DE3) bacteria and the tau was isolated and purified as described [Levy et al., 2005]. The concentration of purified tau was determined by SDS-PAGE comparison with a tau mass standard [Panda et al., 2003].

Kinesin Purification

The kinesin construct used in these studies (K560-GFP-his) was a kind gift from Drs. Andrew Carter and Ron Vale (UC San Francisco). In a pET vector, the cDNA encodes the N-terminal 560 amino acids of human conventional kinesin heavy-chain fused to green fluorescent protein coupled to a C-terminal hexa-his cluster for Ni-affinity purification. K560-GFP-his was expressed in BL21 (DE3). Bacteria were lysed in the presence of protease inhibitors [AEBSF (1 mM), Pepstatin (100 μ g/mL), Leupeptin (100 μ g/mL), Aprotinin (100 μ g/mL)], the lysate was cleared by centrifugation and the resulting supernatant was batch-incubated with Ni-NTA resin (Novagen). The resin-lysate mixture was poured into a fritted column and washed (20 mM imidazole, 50 mM NaH_2PO_4 , 250 mM NaCl, 0.1 mM MgATP, 10 mM β -mercaptoethanol (β -ME), pH 6.0) to reduce nonspecifically bound contaminants. The kinesin fusion protein was eluted with 500 mM imidazole, 50 mM NaH_2PO_4 , 250 mM NaCl, 1 mM MgCl_2 , 0.1 mM MgATP, 10 mM β -ME, pH 7.2 and exchanged into BRB-80 (80 mM Pipes, 1 mM EGTA, 1 mM MgSO_4 , pH 6.8). The kinesin was further purified by a two-step "bind and release" MT-affinity cosedimentation procedure [Case et al., 1997]. The K560-GFP-his (~90–95% pure) was concentrated and stored in BRB-80 supplemented with 10% sucrose and 0.1 mM ATP at -70°C .

Tau-MT Cosedimentation Assays

Fifteen μM tubulin was mixed with purified recombinant 3R or 4R tau at concentrations of 0.5 μM (molar ratio of tau to tubulin of 1:30), 1 μM (molar ratio of 1:15), or 3 μM (molar ratio of 1:5) in BRB-80 buffer with 2 mM GTP. MTs were assembled to steady state at 35°C (1 h), layered over sucrose cushions (50% sucrose in BRB-80, 2 mM GTP), and centrifuged in a Beckman TLA 100.3 fixed angle rotor for 12 min at 35,000 rpm ($52,000 \times g$) at 35°C . Supernatants and pellets were collected and solubilized in SDS-PAGE sample buffer. The quantities of tau and tubulin in each fraction were determined by Western blotting using the monoclonal antibody, tau-1, and Coomassie blue staining respectively, taking care to operate within the linear detection range. Negligible quantities of tau or tubulin remained within the cushion.

Kinesin-Driven MT Gliding Assays

Flow-chambers were constructed by attaching No. 1 glass coverslips to glass microscope slides with double-sided tape. Anti-GFP polyclonal antibodies (Chemicon, AB16901) were adhered to the flow-chamber/coverslip surface by flowing in 5–8 μL of antibody solution (400 $\mu\text{g/mL}$). After 5 min the antibody-coated surface was blocked for an additional 5 min with a solution of 1 mg/mL casein in BRB-80 containing 10 mM β -ME to reduce

nonspecific binding of motors to the glass surface. K560-GFP-his kinesin was then added to the flow-chamber following dilution to 50 $\mu\text{g}/\text{mL}$ in the casein-containing buffer and allowed to adhere for 8 min before washing. To prepare MTs for gliding assays, rhodamine-tubulin was mixed with unlabeled tubulin at a molar ratio of 1:6. Depending on the experiment, MTs were either assembled by addition of tau without any taxol, or by first adding taxol followed by tau. For assembly by taxol, the drug was added in a stepwise fashion over a 15 min period to a final concentration of 20 μM to prevent formation of non-MT structures [Thompson et al., 1981]. MT preparations were clarified by sedimentation through 50% sucrose cushions at 35°C to remove nonpolymerized rhodamine-tubulin, and then diluted to varying extents in a BRB-80 based motility buffer containing 5 mM ATP, 4 mg/mL glucose, 1 μL “Gloxy” [supernatant from a centrifuged mixture of glucose oxidase (7.5 mg), catalase (15 μL), and BRB-80 (35 μL)]. The flow chamber was prewarmed to 35°C on a heating block before addition of the MTs. Fifteen to twenty microliters of the MT/ATP mixture was then applied to the kinesin-containing flow chamber and the chamber was sealed with a mixture of vaseline, lanolin, and paraffin (weight ratios of 1:1:1) prior to imaging. Dilution factors for each MT-assembly condition were optimized to attain the desired MT-density of ~ 5 –25 MTs per field for microscopy and tracking. As a positive control for gliding assay system components, tau-free, taxol-assembled MTs were prepared daily and tracked in parallel with the tau-assembled taxol-free MTs. Gliding data for tau-assembled MTs were analyzed only when the gliding velocity of taxol-stabilized MTs deviated from the standard taxol control mean by less than 5%. Approximately 20–25 MTs were assayed per condition, and data was collected from multiple independent experiments.

Gliding Assay Microscopy, Tracking, and Analysis

Kinesin-driven MT gliding was visualized at 100 \times magnification by selecting for rhodamine excitation at 460 nm using a Nikon Eclipse E800 fluorescence microscope coupled to a Hamamatsu Orca II digital camera. Gliding assays were carried out in a temperature-controlled (35°C) chamber. Each time-series image stack represents a maximum of 120 s, acquired using Metamorph software (Molecular Devices) at 4 s intervals with 100 ms exposure, without binning. For postacquisition data analysis, custom-designed, semiautomated tracking software was developed (Matlab) to locate entire MT-bodies through an image time series and simultaneously collect gliding velocity, trajectory curvature and MT lengths [Sargin et al. 2007, 2008]. Briefly, MTs to be tracked were selected by the experimenter in the first frame in which both ends were visible, and the MT body was automatically seg-

mented using a graph-based search algorithm initiated by a single user-defined point along the MT body [Sargin et al., 2007]. In each subsequent frame, the MT body was tracked by deforming a trellis centered on the previous frame, thereby making the algorithm robust to gliding intersection events [Sargin et al., 2008]. The program enabled the user to correct occasional erroneous tracks manually, which would then be used as more accurate “priors” for automated tracking through subsequent frames. Tracking was terminated when any part of the MT body exited the field of view. Supporting Information movie 1 demonstrates user selection, automatic segmentation, and tracking of a gliding MT. Gliding velocity, trajectory curvature, and MT length data were quantified utilizing both MT tip and MT body center of mass position data. We quantified the curvature of MT gliding trajectory (k) with the following expression:

$$k = \frac{x'y'' - y'x''}{(x'^2 + y'^2)^{3/2}}$$

where (x', y') and (x'', y'') represent coordinates of successive tracked points along the MT trajectory plot. Gaussian curves were fit to gliding velocity histograms using the following expression:

$$\frac{1}{\sigma\sqrt{2\pi}} \exp\left(-\frac{(x - \mu)^2}{2\sigma^2}\right)$$

where x = measured velocity, μ = mean velocity, σ = standard deviation, and σ^2 = variance.

Results

Characterization of Tau Binding to Tau-Assembled and Taxol-Assembled MTs

We first sought to characterize the MTs to be used in our gliding assays. We chose three different initial tau:tubulin ratios, 1:30, 1:15, and 1:5, which bracket the estimated ratio of tau to tubulin found in neurons [Binder et al., 1985; Drubin et al., 1985], and used cosedimentation assays to determine the molar ratios of tau:tubulin bound

Table I. Tau:Tubulin Molar Ratios in Assembled Microtubules

Initial tau:tubulin molar ratio	MT molar ratio (tau:tubulin)	Molecules tau per μm MT length
4R 1:5	1:6	273
4R 1:15	1:17	96
4R 1:30	1:26	63
3R 1:5	1:4	406
3R 1:15	1:9	181
3R 1:30	1:16	102

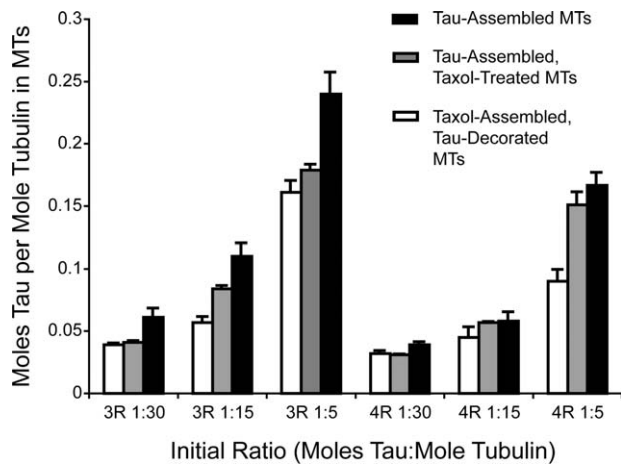


Fig. 2. Taxol reduces the tau:tubulin molar ratio in MT polymers. MTs were assembled in the presence of 3R or 4R tau at the initial tau:tubulin molar ratios shown. Following assembly, MTs were collected by centrifugation and the molar ratio of tau:tubulin in the polymers was quantified. Preassembly of MTs with taxol resulted in lower tau:tubulin ratios in the polymers (white bars) relative to assembly of MTs in the absence of taxol (black bars). Treatment of tau-assembled MTs with taxol (grey bars) resulted in intermediate ratios of tau:tubulin in the MT polymers.

to MTs assembled at these ratios. As shown in Table I, an initial molar ratio of 3R tau to tubulin of 1:30 resulted in a MT-bound ratio of 1:16 moles of tau per mol tubulin, corresponding to 102 molecules of tau per μm of MT length (based on 1639 tubulin dimers per μm of MT length; Table I). It is expected that the ratio of tau bound to the MTs will be greater than the ratio of tau to tubulin in the starting solution because tau binds strongly to MTs but not to free tubulin dimers, and some tubulin remains in solution. At an initial tau:tubulin ratio of 1:15, the ratio of tau to tubulin in the MTs was 1:9 (181 molecules of tau per μm of MT length) and at a ratio of 1:5 mol of tau per mol tubulin in the assembly reactions, the MT-bound molar ratio of tau to tubulin was 1:4, or 406 molecules of tau per μm of MT length. When MTs were assembled with 4R tau at an initial molar ratio of tau to tubulin of 1:30, the ratio of tau to tubulin bound to the MTs was 1:26, or 63 molecules of tau per μm of MT length. At an initial tau:tubulin ratio of 1:15, the ratio of tau to tubulin in the MTs was 1:17 (96 molecules of tau per μm of MT length) and at a ratio of 1:5 mol of tau per mol tubulin in the assembly reaction, the MT-bound molar ratio of tau to tubulin was 1:6, or 273 molecules of tau per μm of MT length. Thus at equivalent initial starting concentrations MTs assembled with 4R tau had somewhat less tau per unit of MT length than those assembled with 3R tau, probably reflecting the stronger MT binding affinity of 4R tau relative to 3R tau and the increased amount of MT polymers formed in the presence of 4R tau.

To the best of our knowledge, all previous investigations of the effects of tau on kinesin-driven MT gliding in vitro

utilized taxol-stabilized MTs. In view of the possible effects that taxol might exert upon tau binding to MTs, we also wanted to determine the stoichiometry of 3R tau and 4R tau binding to MTs that had first been assembled with 20 μM taxol, and to MTs that were first assembled with tau and then treated with 20 μM taxol. As shown in Fig. 2, preassembly of MTs by taxol reduced subsequent binding to the MTs of both 3R and 4R tau, consistent with earlier studies [Kar et al., 2003; Park et al., 2008]. Inhibition of tau binding to MTs was strongest at the highest initial molar ratio of tau to tubulin (1:5), reducing the amount of MT-bound tau to molar ratios of 1:9 from 1:4 and to 1:11 from 1:6 for 3R and 4R tau, respectively (Fig. 2).

We also wanted to know whether taxol could reduce tau binding to MTs when the MTs were assembled with tau prior to adding taxol. Indeed, addition of taxol to tau-assembled MTs also reduced binding of both tau isoforms to the MTs. However, the reduction was less than what occurred when MTs were assembled with taxol prior to addition of tau (Fig. 2). The reduction of 3R tau binding to MTs caused by addition of 20 μM taxol after tau-induced assembly was $\sim 24\%$ when compared to MTs assembled by 3R tau alone. In contrast, the reduction of 4R tau binding to MTs caused by addition of taxol after tau-induced assembly averaged $\sim 13\%$ when compared to MTs assembled by 4R tau alone. Taken together, these data reveal that the amount of tau that can bind to MTs depends upon the assembly conditions and that both pre-assembly with taxol and addition of taxol after tau-induced assembly reduces tau binding to the MTs.

MTs Assembled with Tau Do Not Undergo Detectable Dynamic Instability Behavior During Gliding

MTs, especially MAP-free MTs, undergo extensive growth and shortening [Mitchison and Kirschner, 1984]. In contrast, taxol-assembled MTs exhibit virtually no length changes [Derry et al., 1995], which is why taxol-stabilized MTs are routinely used for in vitro assays of motor activity. In order to analyze MT gliding with MTs assembled

Table II. Length of Gliding Microtubules

Initial tau:tubulin molar ratio	Avg MT length (μm)	Avg Δ MT length ($\mu\text{m} \pm \text{SEM}$)	Avg Δ MT length (%)
4R 1:5	11.4	0.21 ± 0.010	2.2
4R 1:15	10.6	0.21 ± 0.020	2.8
4R 1:30	17.3	0.22 ± 0.012	1.9
3R 1:5	12.4	0.25 ± 0.010	2.3
3R 1:15	11.3	0.22 ± 0.010	2.2
3R 1:30	13.9	0.20 ± 0.015	1.7
Taxol	12.5	0.36 ± 0.013	3.8

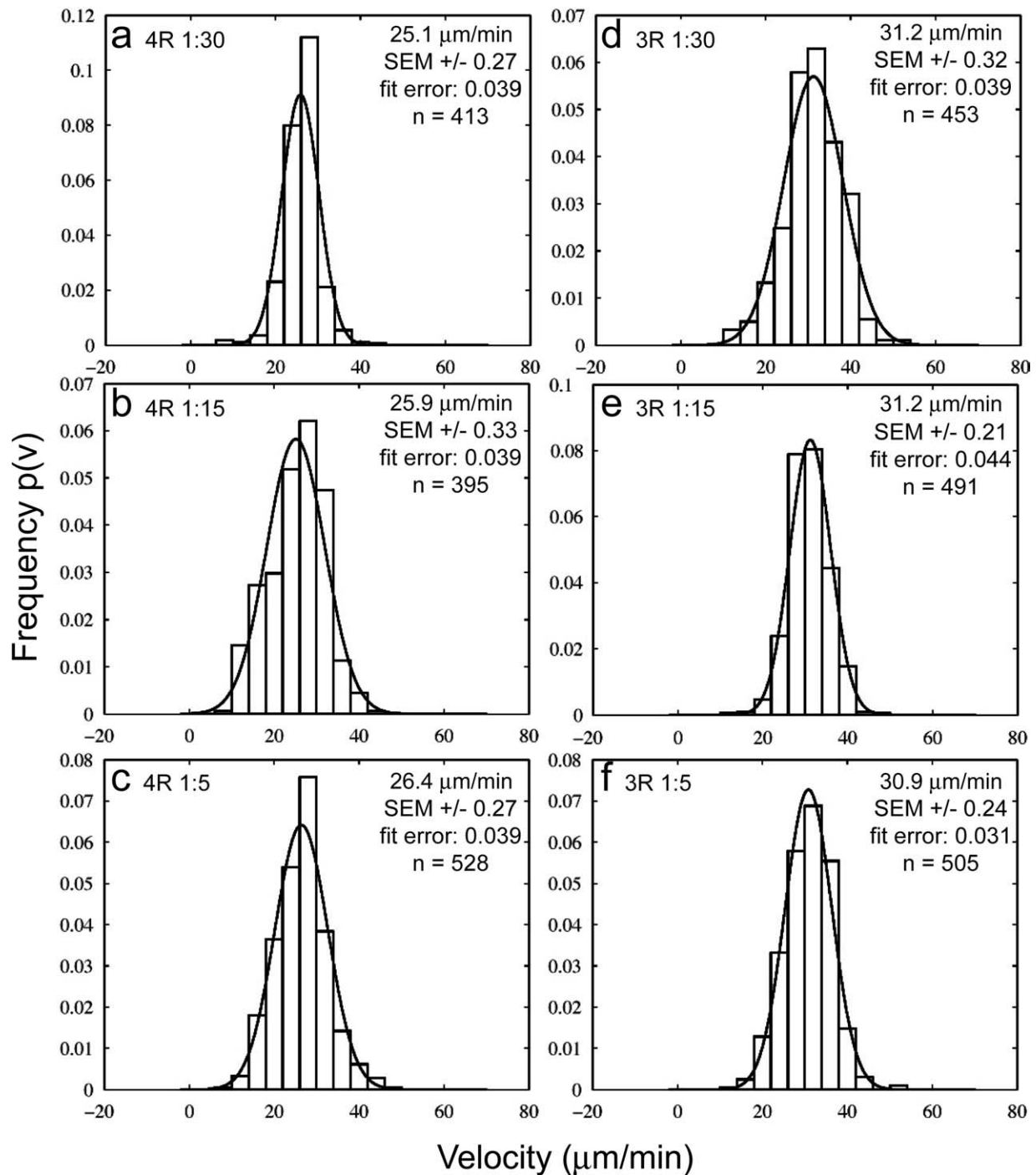


Fig. 3. Tau isoform-specific MT gliding velocities. Panels a–c: Histograms of gliding velocities, binned in 5 μm/min increments, for 4R-assembled MTs at tau:tubulin molar ratios of 1:30, 1:15, and 1:5, respectively. Panels d–f: Histograms of gliding velocities for 3R-assembled MTs at tau:tubulin molar ratios of 1:30, 1:15, and 1:5, respectively. For all conditions, “*n*” refers to number of velocity measurements, with an average of 20 measurements per gliding MT. Gaussian fit errors were approximately equivalent for each group, and all groups demonstrated a single-population distribution of velocity measurements. Within each three-concentration isoform group (a–c and d–f) average gliding velocities deviated from the isoform group mean by less than 3% (4R) and 2% (3R) across a minimum fourfold concentration range.

by tau in the absence of taxol, it was necessary to determine whether the lengths of the tau-stabilized MTs changed during the gliding assays (Materials and Methods), since large MT length changes would make analysis of gliding rates difficult when assayed by tracking tip posi-

tions. As shown in Table II and in Supporting Information Fig. 1, the lengths of the MTs at all three tau-tubulin ratios used in this work varied less than ~3% during the 2 min recording period of the assays. Indeed, tau-stabilized MTs gliding on a kinesin field were less dynamic

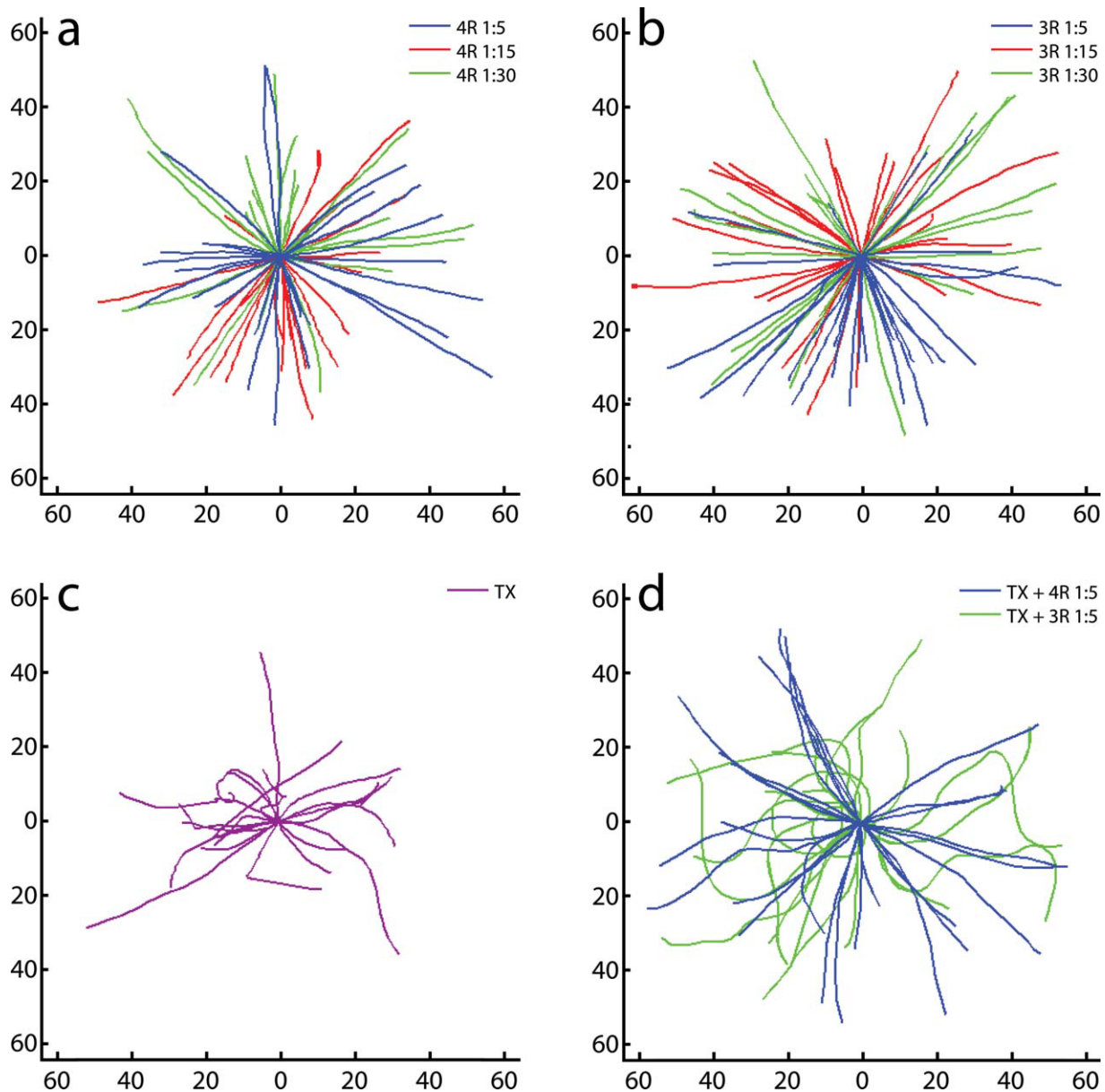


Fig. 4. MT gliding trajectories. Tip positions of gliding MTs were tracked and trajectories were plotted such that the initial points were normalized to a [0,0] origin, with subsequent points radiating outward in arbitrary directions. MTs assembled by 4R (a) and 3R tau (b) exhibit linear gliding. MTs assembled in the presence of taxol display highly curved trajectories (c). Linear gliding of taxol-assembled MTs is restored by decoration with 4R but not 3R tau (d).

than taxol-assembled MTs (Table II). Despite a 7–10-fold dilution of the MTs immediately prior to conducting the gliding assay, there were no catastrophe events detected. The unexpected stability of tau-assembled MTs in the gliding assay may be due to a stabilizing effect of kinesin, as kinesin binding has been shown to stabilize MT protofilaments [Krebs et al., 2004].

3R and 4R Tau Differentially Modulate Kinesin-Driven MT Gliding Velocity

MTs assembled by 4R tau at tau to tubulin molar ratios of 1:30, 1:15, and 1:5 glided at indistinguishable velocities of $25.1 \pm 0.27 \mu\text{m}/\text{min}$, $25.9 \pm 0.33 \mu\text{m}/\text{min}$, and 26.4

$\pm 0.27 \mu\text{m}/\text{min}$ (all SEM), respectively (Figs. 3a–3c). Thus, the 4–5 fold variation in the amount of 4R tau bound to the MTs (between 63 and 273 molecules of tau per μm of MT length) had no effect on gliding velocity. MTs assembled by 3R tau glided at $31.2 \pm 0.32 \mu\text{m}/\text{min}$, $31.2 \pm 0.21 \mu\text{m}/\text{min}$, and $30.9 \pm 0.24 \mu\text{m}/\text{min}$ (all SEM), respectively at added tau to tubulin molar ratios of 1:30, 1:15, and 1:5 (Figs. 3d–3f). As with MTs assembled with 4R tau, the velocity of MTs assembled with 3R tau did not differ among three added tau to tubulin ratios. With 3R tau, the number of tau molecules per μm of MT varied over a fourfold range, between 102 and 406. Most importantly, the 3R tau-assembled MTs glided 17%

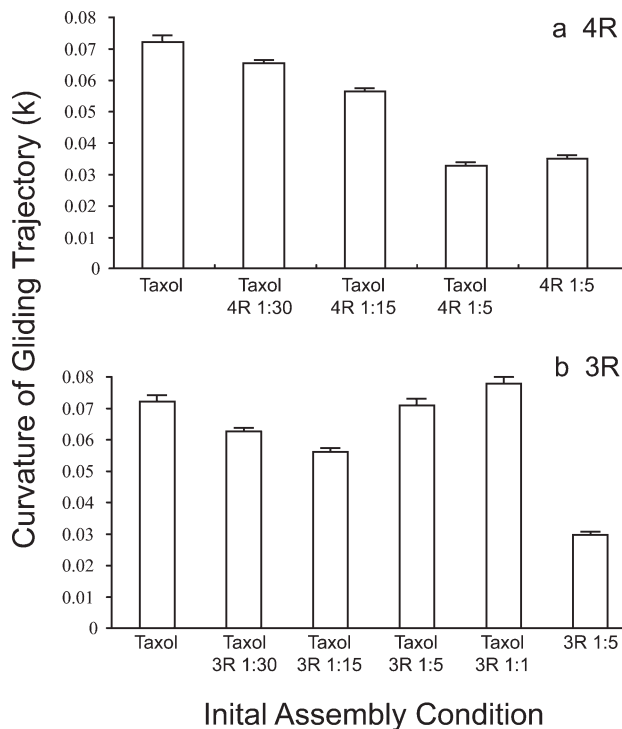


Fig. 5. The curvature of MT gliding trajectories is dependent on assembly conditions. Surface decoration of taxol-assembled MTs by 4R tau restores linear gliding in a concentration-dependent manner (a). In contrast, the gliding trajectories of taxol-assembled MTs decorated with 3R tau remain highly curved (b).

faster than MTs assembled with 4R tau. The faster gliding velocity with 3R tau was highly significant statistically ($P < 0.001$, Student's *t* test). MTs assembled with 20 μM taxol in the absence of any tau glided at a mean velocity of $24.6 \pm 0.34 \mu\text{m}$ per min (SEM; data not shown), which is similar to the velocity of MTs assembled by 4R tau in the absence of taxol.

3R and 4R Tau-Assembled MT Gliding Trajectories

We next analyzed the curvature (*k*) of the paths taken by tau-assembled MTs (i.e., the gliding trajectory). Figure 4 shows gliding trajectory plots with the initial MT tip position normalized to the (0,0) origin and subsequent MT tip positions for each MT radiating outward. MTs assembled by varying ratios of either 3R or 4R tau glided in a linear fashion with very low curvatures (Figs. 4a and 4b; Supporting Information movies 2, 3). More specifically, MTs assembled at 1:30, 1:15, and 1:5 4R tau to tubulin molar ratios exhibited very low curvatures (*k*) of 0.035, 0.045, and 0.035 respectively. Similarly, MTs assembled by 3R tau at the same molar ratios glided with similarly low curvatures (*k*) of 0.027, 0.032, and 0.030, respectively (Fig. 5). Additionally, while tau-assembled MTs glided in a linear fashion, they were capable of transient and

extreme curvature without breaking when encountering obstacles such as debris while gliding (Supporting Information movie 3). Extreme curvature occurred infrequently and the MTs often broke free of the obstacle and resumed linear gliding. Thus, tau-assembled MTs retained the ability to make sharp turns without breaking.

In contrast to the straight gliding trajectories observed with tau-assembled MTs, MTs assembled by taxol glided with curved trajectories, consistent with previous work [Amos and Amos, 1991; Dye et al., 1993; van den Heuvel et al., 2007] (Figs. 4c and 5: $k = 0.072$, Supporting Information movie 4). Furthermore, addition of 4R tau to taxol-assembled MTs restored linear gliding in a concentration-dependent manner (Figs. 4d and 5a). Specifically, taxol-assembled MTs, subsequently decorated with 4R tau at molar ratios of 1:30, 1:15, and 1:5, glided with curvatures (*k*) of 0.065, 0.056, and 0.033, respectively. Thus, at the highest molar ratio of tau to tubulin assayed, the curvature values of taxol-assembled, 4R tau-decorated MTs were similar to MTs assembled with 4R tau in the absence of taxol (Supporting Information movie 5). In contrast, addition of 3R tau to taxol-assembled MTs did not restore linear gliding (Figs. 4d and 5b; Supporting Information movie 6). MTs assembled by taxol and decorated with 3R tau at molar ratios of 1:30, 1:15, and 1:5 glided with high curvatures (*k*) of 0.063, 0.056, and 0.071, respectively. In fact, MTs assembled with taxol and saturated with 3R tau (1:1 molar ratio of tau to tubulin) exhibited gliding trajectories with the highest curvature of all conditions assayed (Fig. 5b, $k = 0.078$).

Discussion

We have analyzed the gliding velocities and gliding trajectories of MTs assembled and stabilized by 3R and 4R tau isoforms rather than traditional MTs assembled and stabilized with high concentrations of taxol. MTs assembled by both 3R and 4R tau, at added ratios of tau to tubulin similar to those found in neurons, underwent minimal dynamic instability when gliding, making them amenable for measuring gliding velocities and trajectories using changes in tip location. 3R tau-assembled MTs containing between 102 and 406 molecules of tau per μm of MT length (1639 tubulin dimers per μm) all glided at the same rate of $\sim 31.1 \mu\text{m/s}$. Thus, the gliding rates were not dependent upon the amount of 3R tau bound to the MT in the range analyzed. MTs assembled with 4R tau, containing between 63 and 276 molecules of tau per μm of MT, all glided at a rate of $\sim 25.9 \mu\text{m/s}$, 17% slower than MTs assembled with 3R tau. While the difference in gliding velocities of MTs assembled with 3R and 4R tau was not large, it was highly significant statistically and relatively modest differences in axonal transport are believed to be of considerable in vivo importance [Morfini et al.,

2009]. MTs assembled with 20 μM taxol in the absence of any tau glided at a mean velocity of 24.6 μm per min, which is similar to the velocity of MTs assembled by 4R tau but not 3R tau. Assembly of MTs stabilized by 3R and 4R tau displayed linear gliding trajectories, although the MTs could still bend, turn, and restraighthen. In contrast, MTs assembled by taxol in the absence of tau displayed highly curved gliding trajectories. Interestingly, addition of 4R tau but not 3R tau to taxol-stabilized MTs restored linear gliding, demonstrating another tau isoform-specific effect.

Use of MTs Stabilized by Taxol versus MTs Stabilized by Tau

The results described here indicate that assembly and stabilization of MTs by tau provide a MT substrate for motor-driven gliding that is as good as, perhaps better than, and certainly different than MTs assembled and stabilized by taxol. A concern about using MTs stabilized by high taxol concentrations as substrates for motors is that taxol changes the protofilament organization and the flexibility of MTs [Dye et al., 1993; Felgner et al., 1996; Diaz et al., 1998; Xiao et al., 2006] and such changes could mask or otherwise affect features of the MT surface important in motor activity and its regulation. Clearly kinesin moves at the same rate on taxol-stabilized and 4R tau-stabilized MTs, thus tau-stabilized MTs are a good substitute for taxol-stabilized MTs in terms of measuring general features of gliding velocities over lawns of kinesin. While past work has shown that addition of tau to taxol-stabilized MTs appears to have little effect on kinesin-translocation velocity [Drubin et al., 1984; Binder et al., 1985; Lopez and Sheetz, 1993; Seitz et al., 2002; Morfini et al., 2007; Vershinin et al., 2007; Dixit et al., 2008], MTs made with 3R tau in the absence of taxol glide 17% faster than taxol-stabilized MTs. This difference could indicate that the use of taxol-stabilized MTs might mask subtle differences between tau isoforms that may be important for tau function in axonal transport. A more striking difference between taxol-stabilized and tau-stabilized MTs is that MTs made with taxol glide with high curvature, while MTs assembled and stabilized by 3R and 4R tau glide linearly. These differences further support a large body of data indicating that the structure or surface topography of taxol-stabilized MTs is different than that of tau-stabilized MTs [Dye et al., 1993; Felgner et al., 1997; Choi et al., 2009]. Such differences in flexural rigidity of the motor substrate (i.e., MTs) could also mask important features of motor-driven transport.

Differential Regulation of Kinesin-Driven MT Gliding Velocity by 3R and 4R Tau

This is the first direct comparison of the effects on kinesin-driven gliding of 3R and 4R tau on nontaxol-stabilized

MTs, and has been carried out with tau isoforms that have the same projection domain. Because 3R and 4R tau, possessing the same N-terminal projection domain, have been shown (i) to possess different abilities to bind to and induce assembly of MTs [Goedert et al., 1990; Goode and Feinstein, 1994; Goode et al., 2000] and (ii) to differentially modulate MT dynamic instability [Trinczek et al., 1995; Panda et al., 2003; Bunker et al., 2004; Levy et al., 2005], this work indicates that the 31 amino acid residues that distinguish the actions of 3R tau and 4R tau might also differentially influence kinesin-driven motility. One might expect that different densities of the tau projection domains might be responsible for the different gliding velocities of MTs made with 3R and 4R tau. However, this seems not to be the case here. MTs assembled and stabilized with 3R tau glided with statistically indistinguishable velocities at all tau:tubulin ratios examined, despite the fact that the MTs had different amounts of bound tau per tubulin dimer. The same was true for 4R tau. Taken together, these data suggest that 3R tau and 4R tau, due to differences in the way they bind to the MT surface, facilitate kinesin-driven MT gliding differently, possibly by altering MT structure or surface topography in isoform-specific manners.

The finding that MTs assembled by 3R tau glide 17% faster than MTs assembled by 4R tau could have important *in vivo* implications. For example, it is possible that motor-driven vesicle transport during development of the fetal nervous system, when only 3R tau is expressed, needs to be faster than in adult neurons which express an approximately 50:50 ratio of 3R and 4R tau. The magnitude of the kinesin translocation rate difference could also be modulated *in vivo* by mechanisms such as tau phosphorylation and/or other interacting proteins. It is also possible that isoform-specific differences between 3R and 4R tau could be related to how aberrant 3R:4R tau expression ratios cause neuronal cell death and dementia in FTDP-17 and related tauopathies. The data are consistent with current notions that errors in axonal transport may underlie many neurodegenerative processes [Saxton et al., 1991; Ferreira et al., 1992; Hurd et al., 1996; Ebner et al., 1998; Tanaka et al., 1998; Trinczek et al., 1999; LaMonte et al., 2002; Stamer et al., 2002; Mandelkowitz et al., 2003; Kieran et al., 2005; Stokin et al., 2005].

Effect of Tau-Mediated MT-Assembly on MT Gliding Trajectories

MT curvature during motor-driven MT gliding is believed to relate to the rigidity of a MT. The idea is that a momentarily free leading MT end “steers” the MT as it glides [van den Heuvel et al., 2007]. By tracking the gliding trajectories of MTs assembled by either 4R or 3R tau in the absence of taxol, we found that MTs assembled with both isoforms glide in a similarly linear fashion (Fig. 4).

Previous work has demonstrated that treatment of MTs with subsaturating levels of tau (in the absence of taxol) increases the flexural rigidity of MTs in a manner that suggests a threshold effect, i.e., 80% of the maximal stiffening is observed at only ~20% of tau saturation [Felgner et al., 1997]. Our finding that both 3R and 4R tau-assembled MTs glide with linear trajectories at the lowest tested tau:tubulin polymer molar ratios (1:16 tau:tubulin for 3R tau and 1:26 for 4R tau) is consistent with a threshold for MT stiffening by tau. These data suggest that tau induces structural changes not only in the tubulin to which it is bound, but also in neighboring tubulins in the MT lattice, thereby allosterically changing the structure or surface topography of the MT along its length. The existence of a threshold for tau-induced MT rigidity is also consistent with earlier work demonstrating that tau-mediated regulation of MT dynamics occurs at tau:tubulin ratios as low as one molecule of tau per several hundred molecules of tubulin [Panda et al., 1995]. The data also indicate that the ability of 4R tau but not 3R tau to restore linear gliding to taxol-assembled MTs must result, directly or indirectly, from the 4R tau-specific 31 amino acid insert in the 4R tau MT binding repeat domain.

Other Limitations of Using Taxol-Stabilized MTs to Study the Effects of Tau on Kinesin-Driven Gliding

As described earlier, evidence exists that tau can bind to two distinct sites on MTs [Serrano et al., 1985; Melki et al., 1991; Redeker et al., 1992; Boucher et al., 1994; Hagiwara et al., 1994; Marya et al., 1994; Maccioni et al., 1995; Nogales et al., 1995; Saoudi et al., 1995; Chau et al., 1998; Al-Bassam et al., 2002; Kar et al., 2003; Makrides et al., 2004]. One site resides on the inside of the MT cylinder proximal to the taxol binding site [Nogales et al., 1995; Kar et al., 2003] and the other corresponds to the acidic C-termini of the tubulins on the MT outer surface [Serrano et al., 1985; Melki et al., 1991; Redeker et al., 1992; Marya et al., 1994; Maccioni et al., 1995; Chau et al., 1998]. A number of biochemical studies also indicate that taxol and tau may directly compete for binding to MTs [Kar et al., 2003; Park et al., 2008]. Further, tau and taxol modulate MT dynamic instability in markedly similar manners [Derry et al., 1995; Panda et al., 1995; Panda et al., 2003; Bunker et al., 2004; Levy et al., 2005], suggesting a possible functional overlap that could stem from occupying the same location in the MT. We found that addition of taxol to MTs, either before or after addition of tau, led to reduced levels of tau in the assembled MTs. Given that tau and taxol might bind to a common region of the MT, a simple conclusion would be that direct competition occurs between taxol and tau for the same or overlapping MT binding sites. These considerations add further weight to

the idea that studying the action of tau on motor-driven gliding with taxol-stabilized MTs may mask certain features of tau action on motor activity.

Conclusions

In summary, using kinesin driven MT gliding as an assay, our data suggest that MTs assembled by 3R and 4R tau possess distinct surface topographies or other structural properties that influence kinesin translocation. These differences could have great in vivo relevance given the importance of MTs and axonal transport for the development and maintenance of the nervous system as well as their roles in numerous neurodegenerative conditions. While beyond the scope of this work, it will be valuable to determine the extent to which 3R and 4R tau might differentially modulate kinesin-driven movement along tau-stabilized MTs using single molecule analysis.

Acknowledgments

The authors thank Mr. Herb Miller for providing purified bovine tubulin and Dr. Kathy Kamath for guidance in microscopy, tubulin rhodamine-labeling, and critical analysis of data. The authors also thank Drs. Andrew Carter and Ron Vale for supplying reagents and expertise on gliding assays. They also thank Drs. Mary Ann Jordan and Megan Valentine for valuable discussions and suggestions. This work was supported by NIH grants NS-13560 (LW), NS-35010 (SCF), NSF grant ITR-0331697 (KR, BSM, SCF and LW), and a grant from CurePSP (SCF and LW).

References

- Al-Bassam J, Ozer RS, Safer D, Halpain S, Milligan RA. 2002. MAP2 and tau bind longitudinally along the outer ridges of microtubule protofilaments. *J Cell Biol* 157(7):1187–1196.
- Amos LA, Amos WB. 1991. The bending of sliding microtubules imaged by confocal light microscopy and negative stain electron microscopy. *J Cell Sci Suppl* 14:95–101.
- Ballatore C, Lee VM, Trojanowski JQ. 2007. Tau-mediated neurodegeneration in Alzheimer's disease and related disorders. *Nat Rev Neurosci* 8(9):663–672.
- Binder LI, Frankfurter A, Rebhun LI. 1985. The distribution of tau in the mammalian central nervous system. *J Cell Biol* 101(4):1371–1378.
- Boucher D, Larcher JC, Gros F, Denoulet P. 1994. Polyglutamylation of tubulin as a progressive regulator of in vitro interactions between the microtubule-associated protein Tau and tubulin. *Biochemistry* 33(41):12471–12477.
- Bunker JM, Wilson L, Jordan MA, Feinstein SC. 2004. Modulation of microtubule dynamics by tau in living cells: implications for development and neurodegeneration. *Mol Biol Cell* 15(6):2720–2728.
- Butner KA, Kirschner MW. 1991. Tau protein binds to microtubules through a flexible array of distributed weak sites. *J Cell Biol* 115(3):717–730.

- Case RB, Pierce DW, Hom-Booher N, Hart CL, Vale RD. 1997. The directional preference of kinesin motors is specified by an element outside of the motor catalytic domain. *Cell* 90(5):959–966.
- Chau MF, Radeke MJ, de Ines C, Barasoain I, Kohlstaedt LA, Feinstein SC. 1998. The microtubule-associated protein tau cross-links to two distinct sites on each alpha and beta tubulin monomer via separate domains. *Biochemistry* 37(51):17692–17703.
- Chen J, Kanai Y, Cowan NJ, Hirokawa N. 1992. Projection domains of MAP2 and tau determine spacings between microtubules in dendrites and axons. *Nature* 360(6405):674–677.
- Choi MC, Raviv U, Miller HP, Gaylord MR, Kiris E, Ventimiglia D, Needleman DJ, Kim MW, Wilson L, Feinstein SC, Safinya CR. 2009. Human microtubule-associated-protein tau regulates the number of protofilaments in microtubules: a synchrotron x-ray scattering study. *Biophys J* 97(2):519–527.
- Derry WB, Wilson L, Jordan MA. 1995. Substoichiometric binding of taxol suppresses microtubule dynamics. *Biochemistry* 34(7):2203–2211.
- Diaz JF, Valpuesta JM, Chacon P, Diakun G, Andreu JM. 1998. Changes in microtubule protofilament number induced by Taxol binding to an easily accessible site. *Internal microtubule dynamics. J Biol Chem* 273(50):33803–33810.
- Dixit R, Ross JL, Goldman YE, Holzbaur EL. 2008. Differential regulation of dynein and kinesin motor proteins by tau. *Science* 319(5866):1086–1089.
- Drubin DG, Caput D, Kirschner MW. 1984. Studies on the expression of the microtubule-associated protein, tau, during mouse brain development, with newly isolated complementary DNA probes. *J Cell Biol* 98(3):1090–1097.
- Drubin DG, Feinstein SC, Shooter EM, Kirschner MW. 1985. Nerve growth factor-induced neurite outgrowth in PC12 cells involves the coordinate induction of microtubule assembly and assembly-promoting factors. *J Cell Biol* 101(5 Pt 1):1799–1807.
- Duncan JE, Goldstein LS. 2006. The genetics of axonal transport and axonal transport disorders. *PLoS Genet* 2(9):e124; doi: 10.1371/journal.pgen.0020124.
- Dye RB, Fink SP, Williams RC, Jr. 1993. Taxol-induced flexibility of microtubules and its reversal by MAP-2 and Tau. *J Biol Chem* 268(10):6847–6850.
- Ebneth A, Godemann R, Stamer K, Illenberger S, Trinczek B, Mandelkow E. 1998. Overexpression of tau protein inhibits kinesin-dependent trafficking of vesicles, mitochondria, and endoplasmic reticulum: implications for Alzheimer's disease. *J Cell Biol* 143(3):777–794.
- Feinstein SC, Wilson L. 2005. Inability of tau to properly regulate neuronal microtubule dynamics: a loss-of-function mechanism by which tau might mediate neuronal cell death. *Biochim Biophys Acta* 1739(2–3):268–279.
- Felgner H, Frank R, Schliwa M. 1996. Flexural rigidity of microtubules measured with the use of optical tweezers. *J Cell Sci* 109(Pt 2):509–516.
- Felgner H, Frank R, Biernat J, Mandelkow EM, Mandelkow E, Ludin B, Matus A, Schliwa M. 1997. Domains of neuronal microtubule-associated proteins and flexural rigidity of microtubules. *J Cell Biol* 138(5):1067–1075.
- Ferreira A, Niclas J, Vale RD, Banker G, Kosik KS. 1992. Suppression of kinesin expression in cultured hippocampal neurons using antisense oligonucleotides. *J Cell Biol* 117(3):595–606.
- Goedert M, Jakes R. 1990. Expression of separate isoforms of human tau protein: correlation with the tau pattern in brain and effects on tubulin polymerization. *Embo J* 9(13):4225–4230.
- Goode BL, Feinstein SC. 1994. Identification of a novel microtubule binding and assembly domain in the developmentally regulated inter-repeat region of tau. *J Cell Biol* 124(5):769–782.
- Goode BL, Chau M, Denis PE, Feinstein SC. 2000. Structural and functional differences between 3-repeat and 4-repeat tau isoforms. Implications for normal tau function and the onset of neurodegenerative disease. *J Biol Chem* 275(49):38182–38189.
- Hagiwara H, Yorifuji H, Sato-Yoshitake R, Hirokawa N. 1994. Competition between motor molecules (kinesin and cytoplasmic dynein) and fibrous microtubule-associated proteins in binding to microtubules. *J Biol Chem* 269(5):3581–3589.
- Himmler A. 1989. Structure of the bovine tau gene: alternatively spliced transcripts generate a protein family. *Mol Cell Biol* 9(4):1389–1396.
- Himmler A, Drechsel D, Kirschner MW, Martin DW, Jr. 1989. Tau consists of a set of proteins with repeated C-terminal microtubule-binding domains and variable N-terminal domains. *Mol Cell Biol* 9(4):1381–1388.
- Hirokawa N, Shiomura Y, Okabe S. 1988. Tau proteins: the molecular structure and mode of binding on microtubules. *J Cell Biol* 107(4):1449–1459.
- Hurd DD, Stern M, Saxton WM. 1996. Mutation of the axonal transport motor kinesin enhances paralytic and suppresses shaker in *Drosophila*. *Genetics* 142(1):195–204.
- Hyman A, Drechsel D, Kellogg D, Salser S, Sawin K, Steffen P, Wordeman L, Mitchison T. 1991. Preparation of modified tubulins. *Methods Enzymol* 196:478–485.
- Kar S, Fan J, Smith MJ, Goedert M, Amos LA. 2003. Repeat motifs of tau bind to the insides of microtubules in the absence of taxol. *Embo J* 22(1):70–77.
- Keskin O, Durell SR, Bahar I, Jernigan RL, Covell DG. 2002. Relating molecular flexibility to function: a case study of tubulin. *Biophys J* 83(2):663–680.
- Kieran D, Hafezparast M, Bohnert S, Dick JR, Martin J, Schiavo G, Fisher EM, Greensmith L. 2005. A mutation in dynein rescues axonal transport defects and extends the life span of ALS mice. *J Cell Biol* 169(4):561–567.
- Kosik KS, Orecchio LD, Bakalis S, Neve RL. 1989. Developmentally regulated expression of specific tau sequences. *Neuron* 2(4):1389–1397.
- Krebs A, Goldie KN, Hoenger A. 2004. Complex formation with kinesin motor domains affects the structure of microtubules. *J Mol Biol* 335(1):139–153.
- LaMonte BH, Wallace KE, Holloway BA, Shelly SS, Ascano J, Tokito M, Van Winkle T, Howland DS, Holzbaur EL. 2002. Disruption of dynein/dynactin inhibits axonal transport in motor neurons causing late-onset progressive degeneration. *Neuron* 34(5):715–727.
- Lee G, Cowan N, Kirschner M. 1988. The primary structure and heterogeneity of tau protein from mouse brain. *Science* 239(4837):285–288.
- Lee VM, Goedert M, Trojanowski JQ. 2001. Neurodegenerative tauopathies. *Annu Rev Neurosci* 24:1121–1159.
- Levy SF, Leboeuf AC, Massie MR, Jordan MA, Wilson L, Feinstein SC. 2005. Three- and four-repeat tau regulate the dynamic instability of two distinct microtubule subpopulations in qualitatively different manners. Implications for neurodegeneration. *J Biol Chem* 280(14):13520–13528.
- Lopez LA, Sheetz MP. 1993. Steric inhibition of cytoplasmic dynein and kinesin motility by MAP2. *Cell Motil Cytoskeleton* 24(1):1–16.

- Maccioni RB, Tapia L, Cambiazo V. 1995. Functional organization of tau proteins during neuronal differentiation and development. *Braz J Med Biol Res* 28(8):827–841.
- Makrides V, Massie MR, Feinstein SC, Lew J. 2004. Evidence for two distinct binding sites for tau on microtubules. *Proc Natl Acad Sci USA* 101(17):6746–6751.
- Mandelkow EM, Stamer K, Vogel R, Thies E, Mandelkow E. 2003. Clogging of axons by tau, inhibition of axonal traffic and starvation of synapses. *Neurobiol Aging* 24(8):1079–1085.
- Marya PK, Syed Z, Fraylich PE, Eagles PA. 1994. Kinesin and tau bind to distinct sites on microtubules. *J Cell Sci* 107(Pt 1): 339–344.
- Melki R, Kerjan P, Waller JP, Carlier MF, Pantaloni D. 1991. Interaction of microtubule-associated proteins with microtubules: yeast lysyl- and valyl-tRNA synthetases and tau 218-235 synthetic peptide as model systems. *Biochemistry* 30(49):11536–11545.
- Miller HP, Wilson L. 2010. Preparation of microtubule protein and purified tubulin from bovine brain by cycles of assembly and disassembly and phosphocellulose chromatography. In: Wilson L, Correia JJ, editors. *Methods in Cell Biology*. Elsevier Inc. Vol 95; p 3–15.
- Mitchison T, Kirschner M. 1984. Dynamic instability of microtubule growth. *Nature* 312(5991):237–242.
- Morfini G, Pigino G, Mizuno N, Kikkawa M, Brady ST. 2007. Tau binding to microtubules does not directly affect microtubule-based vesicle motility. *J Neurosci Res* 85(12):2620–2630.
- Morfini GA, Burns M, Binder LI, Kanaan NM, LaPointe N, Bosco DA, Brown RH, Jr., Brown H, Tiwari A, Hayward L, et al. 2009. Axonal transport defects in neurodegenerative diseases. *J Neurosci* 29(41):12776–12786.
- Muto E, Sakai H, Kaseda K. 2005. Long-range cooperative binding of kinesin to a microtubule in the presence of ATP. *J Cell Biol* 168(5):691–696.
- Nogales E, Wolf SG, Khan IA, Luduena RF, Downing KH. 1995. Structure of tubulin at 6.5 Å and location of the taxol-binding site. *Nature* 375(6530):424–427.
- Panda D, Goode BL, Feinstein SC, Wilson L. 1995. Kinetic stabilization of microtubule dynamics at steady state by tau and microtubule-binding domains of tau. *Biochemistry* 34(35):11117–11127.
- Panda D, Samuel JC, Massie M, Feinstein SC, Wilson L. 2003. Differential regulation of microtubule dynamics by three- and four-repeat tau: implications for the onset of neurodegenerative disease. *Proc Natl Acad Sci USA* 100(16):9548–9553.
- Park H, Kim M, Fyngenson DK. 2008. Tau-isoform dependent enhancement of taxol mobility through microtubules. *Arch Biochem Biophys* 478(1):119–126.
- Redeker V, Melki R, Prome D, Le Caer JP, Rossier J. 1992. Structure of tubulin C-terminal domain obtained by subtilisin treatment. The major alpha and beta tubulin isoforms from pig brain are glutamylated. *FEBS Lett* 313(2):185–192.
- Samsonov A, Yu JZ, Rasenick M, Popov SV. 2004. Tau interaction with microtubules in vivo. *J Cell Sci* 117(Pt 25):6129–6141.
- Saoudi Y, Paintrand I, Multigner L, Job D. 1995. Stabilization and bundling of subtilisin-treated microtubules induced by microtubule associated proteins. *J Cell Sci* 108(Pt 1):357–367.
- Sargin ME, Altinok A, Rose K, Manjunath BS. 2007. Tracing curvilinear structures in live cell images. San Antonio, TX: IEEE International Conference on Image Processing, September 16th-19th, 2007. VI-285–VI-288.
- Sargin ME, Altinok A, Rose K, Manjunath BS. 2008. Deformable trellis: open contour tracking in bio-image sequences. Las Vegas, Nevada: IEEE International Conference on Acoustics, Speech and Signal Processing, March 30–April 4, 2008; p 561–564.
- Saxton WM, Hicks J, Goldstein LS, Raff EC. 1991. Kinesin heavy chain is essential for viability and neuromuscular functions in *Drosophila*, but mutants show no defects in mitosis. *Cell* 64(6): 1093–1102.
- Seitz A, Kojima H, Oiwa K, Mandelkow EM, Song YH, Mandelkow E. 2002. Single-molecule investigation of the interference between kinesin, tau and MAP2c. *Embo J* 21(18):4896–4905.
- Serrano L, Montejo de Garcini E, Hernandez MA, Avila J. 1985. Localization of the tubulin binding site for tau protein. *Eur J Biochem* 153(3):595–600.
- Spittaels K, Van den Haute C, Van Dorpe J, Bruynseels K, Vandezande K, Laenen I, Geerts H, Mercken M, Sciot R, Van Lommel A, et al. 1999. Prominent axonopathy in the brain and spinal cord of transgenic mice overexpressing four-repeat human tau protein. *Am J Pathol* 155(6):2153–2165.
- Stamer K, Vogel R, Thies E, Mandelkow E, Mandelkow EM. 2002. Tau blocks traffic of organelles, neurofilaments, and APP vesicles in neurons and enhances oxidative stress. *J Cell Biol* 156(6):1051–1063.
- Stokin GB, Lillo C, Falzone TL, Brusch RG, Rockenstein E, Mount SL, Raman R, Davies P, Masliah E, Williams DS, et al. 2005. Axonopathy and transport deficits early in the pathogenesis of Alzheimer's disease. *Science* 307(5713):1282–1288.
- Tanaka Y, Kanai Y, Okada Y, Nonaka S, Takeda S, Harada A, Hirokawa N. 1998. Targeted disruption of mouse conventional kinesin heavy chain, kif5B, results in abnormal perinuclear clustering of mitochondria. *Cell* 93(7):1147–1158.
- Thompson WC, Wilson L, Purich DL. 1981. Taxol induces microtubule assembly at low temperature. *Cell Motil* 1(4):445–454.
- Trinczek B, Biernat J, Baumann K, Mandelkow EM, Mandelkow E. 1995. Domains of tau protein, differential phosphorylation, and dynamic instability of microtubules. *Mol Biol Cell* 6(12): 1887–1902.
- Trinczek B, Ebner A, Mandelkow EM, Mandelkow E. 1999. Tau regulates the attachment/detachment but not the speed of motors in microtubule-dependent transport of single vesicles and organelles. *J Cell Sci* 112(Pt 14):2355–2367.
- van den Heuvel MG, Bolhuis S, Dekker C. 2007. Persistence length measurements from stochastic single-microtubule trajectories. *Nano Lett* 7(10):3138–3144.
- Vershinin M, Carter BC, Razafsky DS, King SJ, Gross SP. 2007. Multiple-motor based transport and its regulation by Tau. *Proc Natl Acad Sci USA* 104(1):87–92.
- Xiao H, Verdier-Pinard P, Fernandez-Fuentes N, Burd B, Angeletti R, Fiser A, Horwitz SB, Orr GA. 2006. Insights into the mechanism of microtubule stabilization by Taxol. *Proc Natl Acad Sci USA* 103(27):10166–10173.